

Remote recoil: a new wave-mean interaction effect

By OLIVER BÜHLER¹ AND MICHAEL E. MCINTYRE²

¹Center for Atmosphere Ocean Science at the Courant Institute of Mathematical Sciences, New York University, New York, NY 10012, USA

²Centre for Atmospheric Science at the Department of Applied Mathematics and Theoretical Physics, University of Cambridge, Wilberforce Rd., Cambridge CB3 0WA, UK

(Received 1 November 2002 and in revised form 25 April 2003)

We present a theoretical study of a fundamentally new wave-mean or wave-vortex interaction effect able to force persistent, cumulative change in mean flows in the absence of wave breaking or other kinds of wave dissipation. It is associated with the refraction of non-dissipating waves by inhomogeneous mean (vortical) flows. The effect is studied in detail in the simplest relevant model, the two-dimensional compressible flow equations with a generic polytropic equation of state. This includes the usual shallow-water equations as a special case. The refraction of a narrow, slowly varying wavetrain of small-amplitude gravity or sound waves obliquely incident on a single weak (low Froude or Mach number) vortex is studied in detail. It is shown that, concomitant with the changes in the waves' pseudomomentum due to the refraction, there is an equal and opposite recoil force that is felt, in effect, by the vortex core. This effective force is called a 'remote recoil' to stress that there is no need for the vortex core and wavetrain to overlap in physical space. There is an accompanying 'far-field recoil' that is still more remote, as in classical vortex-impulse problems. The remote-recoil effects are studied perturbatively using the wave amplitude and vortex weakness as small parameters. The nature of the remote recoil is demonstrated in various set-ups with wavetrains of finite or infinite length. The effective recoil force \mathbf{R}_V on the vortex core is given by an expression resembling the classical Magnus force felt by moving cylinders with circulation. In the case of wavetrains of infinite length, an explicit formula for the scattering angle θ_* of waves passing a vortex at a distance is derived correct to second order in Froude or Mach number. To this order $\mathbf{R}_V \propto \theta_*$. The formula is cross-checked against numerical integrations of the ray-tracing equations. This work is part of an ongoing study of internal-gravity-wave dynamics in the atmosphere and may be important for the development of future gravity-wave parametrization schemes in numerical models of the global atmospheric circulation. At present, all such schemes neglect remote-recoil effects caused by horizontally inhomogeneous mean flows. Taking these effects into account should make the parametrization schemes significantly more accurate.

1. Introduction

Wave-induced mean forces and the consequent 'gyroscopic pumping' drive global-scale, greenhouse-gas-transporting circulations in the Earth's middle atmosphere, between about 15 and 100 km altitude. In the middle latitudes of the summer hemisphere, for instance, persistent eastward forces mediated by internal gravity

waves pump air equatorwards, through the Coriolis effect, at mesospheric altitudes around 90 km (recent reviews include those of Fritts & Alexander 2003, Kim, Eckermann & Chun 2003, and McIntyre 2003). The resulting polar upwelling supplies water vapour from below and acts as a gigantic natural refrigerator. Despite intense solar radiation, which is maximal at the pole because of the Earth's tilt, temperatures as low as 105 K have been observed in the summer polar cap (Lübben 1999 and references therein). These are by far the lowest of naturally occurring terrestrial temperatures. One of the observable consequences is the formation of 'noctilucent clouds' between 80 and 90 km, a phenomenon first noticed in the late nineteenth century and sometimes argued to be the 'miner's canary' forewarning us of global water-vapour trends associated with climate change (e.g. Thomas *et al.* 1989).

The persistent mean forces producing the mesospheric gyroscopic pumping are thought to be associated with the dissipation of internal gravity waves by breaking; and there are strong arguments, dating back to the work of Palmer, Shutts & Swinbank (1985), indicating that such forces may be significant at far lower altitudes as well. Representation of such forces in global numerical models of the atmosphere, through so-called "parametrization schemes", is standard practice today. Thus, Fritts & Alexander (2003) state that "accurate parameterization... remains a critical need", and Kim *et al.* (2003) state that the gravity-wave parametrizations 'are now critical components of virtually all large-scale atmospheric models'. This is because the models have far less numerical resolution than would be needed to represent the gravity waves directly. However, such parametrizations currently rely on a paradigm from classical wave-mean interaction theories that assume a horizontally homogeneous mean state. This paradigm can be summarized as a 'pseudomomentum rule' stating that persistent mean forces arise only where the waves break or otherwise dissipate, and that the mean forces arising from dissipation can be equated to the rate of dissipation of the wave property known as pseudomomentum, defined as wave action times wavenumber. We show here that the paradigm is incomplete, because it neglects a new and fundamentally different class of wave-induced mean forces, which have no dependence on wave dissipation yet are equally persistent, with cumulative effects.

This new class of wave-induced mean forces depends on horizontal inhomogeneity and is therefore invisible to the classical wave-mean theories (e.g. Eliassen & Palm 1961; Booker & Bretherton 1967; Jones 1967) on which the current paradigm is based. To our surprise, the new forces do not appear to have been studied before, even in idealized cases. They are certainly neglected in all current parametrization schemes, and indeed are beginning to be called the 'missing forces'. This paper presents the first detailed study of such forces, in the simplest possible cases only. The forces arise whenever waves propagate on a mean state that varies in both horizontal dimensions, latitude and longitude, as in the real atmosphere and oceans with their complicated meandering currents and vortices. The simplest problem in which the new forces arise is the scattering of a narrow wavetrain obliquely incident on a single circular vortex (but without restricting attention to azimuthal force components, as in the classical wave-mean theories). This is the problem considered here, for the simplest possible fluid systems (non-rotating shallow-water dynamics and gas dynamics), but emphasizing those features likely to be robust enough to carry over to more realistic cases. The results show that the dynamical mechanisms in play involve what we call 'remote recoil', in two distinct senses simultaneously.

First, the mean state feels an effective force that satisfies an extension of the pseudomomentum rule — that is, the force can be evaluated from the rate of change of the waves' pseudomomentum due to refraction by the vortex — but the force is

felt not where the waves are refracted but, rather, at the vortex core. More precisely, the effect on the vorticity field is the same as if the waves were absent but the mean force were applied to the vortex core. That is what is relevant to the parametrization problem. In the examples to be studied, conditions are such that the waves can be described by ray theory, with the vortex core relatively far away from the refracted ray paths. The effective wave-induced force on the core, thus conceived, will be called the ‘vortex-core recoil’ and denoted by \mathbf{R}_V .

Second, the complete balance of forces — equivalently, the complete momentum budget, as distinct from the pseudomomentum budget — involves a recoil that is still more remote. This is transmitted by a mean pressure field, $O(a^2)$ in wave amplitude a and of dipole form, that extends beyond the region containing the vortex core and the refracted ray paths. It may be called the ‘far-field recoil’. The simplest versions of the problem are those in which the $O(a)$ wave field is considered to be steady. Then the far-field recoil extends to infinity, in the same way as in classical vortex-impulse problems. In more realistic versions that allow unsteady wave fields, the far-field recoil extends out to the furthest $O(a^2)$ acoustic or gravity wavefront.

The free surface of a shallow-water system is the simplest way of idealizing the stable stratification of the atmosphere and oceans, internal gravity waves being replaced by surface gravity waves. Such models are well established as providing useful idealizations of a range of dynamical processes in the atmosphere and oceans, on the understanding that certain features such as nonlinear steepening, which have no direct counterpart for three-dimensional internal gravity waves, are ignored or artificially suppressed (Bühler 1998). One can note in passing that the present work may also have applications in other areas of physics that involve interactions between waves and vortices. An example would be the study of phonons and quantized vortex lines in superfluids such as liquid helium (e.g. Donnelly 1991).

The plan of the paper is as follows. In §2 the governing equations are introduced and the standard ray theory is summarized. In §3 a simple set-up consisting of a wave source and sink but no vortex is introduced in order to describe recoil forces in the absence of refraction. Then, in §4, the vortex is added and the remote recoil effect is discussed for the case of a finite wavetrain. Then §5 treats the scattering of an infinite wavetrain, a problem that demands a higher order of approximation. The theory is cross-checked by numerical ray-tracing computations in §6 and concluding remarks are made in §7.

2. Governing equations and linear waves

The governing equations are the continuity equation

$$\frac{Dh}{Dt} + h\nabla \cdot \mathbf{u} = 0 \quad (2.1)$$

and the momentum equation

$$\frac{D\mathbf{u}}{Dt} + \frac{c_0^2}{\gamma - 1} \nabla(h^{\gamma-1}) = \mathbf{F}. \quad (2.2)$$

As is well known, these equations can be interpreted either as representing two-dimensional nonlinear gas dynamics with γ the ratio of specific heats or polytropic exponent, or, when $\gamma = 2$, as representing the motion of thin fluid layer with a free surface, whose depth h is viewed as the fluid density per unit area, in suitable units. Because of the relevance to atmospheric gravity waves, we shall usually stress the

latter interpretation. Therefore, h is the dimensionless fluid layer depth such that $h=1$ corresponds to an undisturbed layer, $\mathbf{u}=(u, v)$ is the two-dimensional velocity in the (x, y) directions, c_0 is the linear gravity-wave or sound speed for an undisturbed layer, and \mathbf{F} is a body force per unit mass that remains to be specified in various ways in order to model, for instance, wave emission and absorption. The role of the polytropic exponent γ is made clearer by re-writing (2.2) in momentum-flux form as

$$\frac{\partial(h\mathbf{u})}{\partial t} + \nabla \cdot (h\mathbf{u}\mathbf{u}) + \nabla p = h\mathbf{F}, \quad \text{where } p \equiv \frac{c_0^2}{\gamma}h^\gamma, \quad (2.3)$$

which is the ‘pressure’ function that describes the non-advective momentum flux. Different choices for γ correspond only to changes in the nonlinear details of the pressure function $p=p(h)$, since we shall regard c_0 as fixed. Thus, allowing different values of γ in our calculations has the advantage of automatically flagging those results that are sensitive to such nonlinear details of the pressure function, which we find instructive. The case $\gamma=-1$ has special interest in that nonlinear steepening is suppressed (Bühler 1998), which will be useful when thinking about wave sources and sinks ‘at infinity’ as in § 5. Here we ignore an additive constant in p . Of course, there is no simple physical interpretation of $\gamma \neq 2$ for the shallow-water layer under gravity.

The equations will be studied perturbatively correct to three orders in the usual small-wave-amplitude parameter $a \ll 1$, i.e. there will be an $O(1)$ background flow (denoted throughout by \mathbf{U} and H), $O(a)$ waves, and an $O(a^2)$ mean-flow response to the waves. The method will be classical asymptotics to $O(a^2)$ (e.g. Rayleigh 1896; Longuet-Higgins & Stewart 1964; Bretherton 1969), using Eulerian averaging. It will be assumed throughout that the waves form a slowly varying wavetrain, which allows averaging over the rapidly varying wave phase in the usual way, and permits the use of ray theory. This averaging operation decomposes all flow fields ϕ into a mean part $\bar{\phi}$ and a disturbance part ϕ' such that

$$\phi = \bar{\phi} + \phi' \quad \text{and} \quad \overline{(\phi')} = 0 \quad (2.4)$$

holds with negligible error. The use of ray theory will permit clearcut thought experiments in which a narrow wavetrain is incident to one side or other of the vortex core. Such thought experiments best isolate the remote-recoil effects.

2.1. Linear waves and ray tracing

The general $O(a)$ equations of motion describing linear waves $\{\mathbf{u}', h'\}$ on an $O(1)$ background flow $\{\mathbf{U}, H\}$ are

$$\frac{\partial h'}{\partial t} + \nabla \cdot (H\mathbf{u}' + h'\mathbf{U}) = 0, \quad (2.5)$$

$$\frac{\partial \mathbf{u}'}{\partial t} + (\mathbf{U} \cdot \nabla)\mathbf{u}' + (\mathbf{u}' \cdot \nabla)\mathbf{U} + c^2 \nabla h' = \mathbf{F}', \quad (2.6)$$

where the local wave speed $c=c_0\sqrt{H^{\gamma-1}}$. The linearized force \mathbf{F}' per unit mass is specified as irrotational, as is appropriate for representing wave emission and absorption. These equations will be solved using the standard ray-tracing approximation, which is valid for a slowly varying wavetrain embedded in a slowly varying background environment (e.g. Whitham 1974). Thus the wave fields are taken as

$$\{\mathbf{u}', h'\} = \left\{ c \frac{\mathbf{k}}{\kappa}, H \right\} a \cos(\Theta), \quad (2.7)$$

$$\mathbf{k} = \nabla \Theta, \quad \omega = -\frac{\partial \Theta}{\partial t}, \quad (2.8)$$

$$\omega = \hat{\omega} + \mathbf{U} \cdot \mathbf{k}, \quad \hat{\omega} = c\kappa, \quad (2.9)$$

where $\mathbf{k} = (k, l)$ is the local wavenumber vector, ω is the absolute wave frequency, and the intrinsic frequency $\hat{\omega}$ is given in terms of $\kappa = |\mathbf{k}|$ by the dispersion relation in (2.9). Only the phase Θ varies rapidly, whilst the wave amplitude a as well as \mathbf{k} and ω all vary slowly in space and time. The standard ray-tracing equations for $\mathbf{x} = (x, y)$ and $\mathbf{k} = (k, l)$ as functions of time along group-velocity rays are given in terms of the absolute frequency function

$$\Omega(\mathbf{x}, \mathbf{k}, t) = c\kappa + \mathbf{U} \cdot \mathbf{k} \quad (2.10)$$

by Hamilton's equations

$$\frac{d\mathbf{x}}{dt} = +\frac{\partial \Omega}{\partial \mathbf{k}} \quad \text{and} \quad \frac{d\mathbf{k}}{dt} = -\frac{\partial \Omega}{\partial \mathbf{x}}. \quad (2.11)$$

For steady $\{\mathbf{U}, H\}$ the ray-tracing equations imply that $d\omega/dt = 0$, i.e. the absolute frequency is constant along a ray. This will be the case throughout this paper. The group velocity is

$$\mathbf{u}_g = (u_g, v_g) = \frac{d\mathbf{x}}{dt} = c \frac{\mathbf{k}}{\kappa} + \mathbf{U}. \quad (2.12)$$

The time derivative along a ray is equivalent to the operator

$$\frac{d}{dt} = \frac{\partial}{\partial t} + (\mathbf{u}_g \cdot \nabla) \quad (2.13)$$

acting on slowly varying functions of (\mathbf{x}, t) . The explicit evolution equations for $\mathbf{k} = (k, l)$ are

$$\frac{dk}{dt} = -\frac{\partial c}{\partial x} \kappa - \frac{\partial U}{\partial x} k - \frac{\partial V}{\partial x} l \quad \text{and} \quad \frac{dl}{dt} = -\frac{\partial c}{\partial y} \kappa - \frac{\partial U}{\partial y} k - \frac{\partial V}{\partial y} l, \quad (2.14)$$

where $\mathbf{U} = (U, V)$.

The evolution of wave amplitude a along a ray is governed by the standard conservation law for the wave action A at $O(a^2)$ (e.g. Bretherton & Garrett 1968; Whitham 1974),

$$\frac{\partial(HA)}{\partial t} + \nabla \cdot (HA\mathbf{u}_g) = \frac{H}{\hat{\omega}} \overline{\mathbf{u}' \cdot \mathbf{F}'}. \quad (2.15)$$

Here

$$A = \frac{E}{\hat{\omega}} \quad \text{and} \quad E = \overline{|\mathbf{u}'|^2} = c^2 \frac{\overline{h'^2}}{H^2} = c_0^2 H^{\gamma-3} \overline{h'^2} \quad (2.16)$$

is the wave energy per unit mass, which satisfies equipartition in this case as indicated. From $2E = a^2 c^2$ one can hence deduce the amplitude a from a knowledge of A and vice versa.

The scalar wave action is conserved in regions where $\mathbf{F}' = 0$. Another important wave activity measure is given by the *pseudomomentum* vector,

$$\mathbf{p} = \mathbf{k}A = \frac{\overline{h' \mathbf{u}'}}{H} \quad (2.17)$$

per unit mass. It can be shown to satisfy

$$\frac{\partial(H\mathbf{p})}{\partial t} + \nabla \cdot (H\mathbf{p}\mathbf{u}_g) = HA \frac{d\mathbf{k}}{dt} + \overline{h' \mathbf{F}'}, \quad (2.18)$$

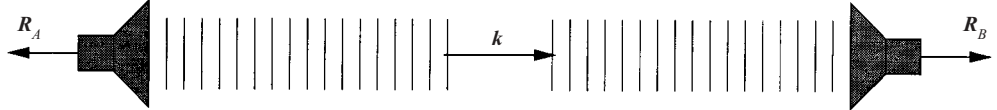


FIGURE 1. A monochromatic wavetrain of length \$2L\$ is emitted by a wave source on the left and absorbed by a wave sink on the right; \$\mathbf{k}\$ is the wavenumber vector. The source and sink feel equal and opposite mean \$O(a^2)\$ recoil forces \$\mathbf{R}_A\$ and \$\mathbf{R}_B\$, respectively. In place of the mechanical wavemakers iconized here, the theoretical analysis uses artificial irrotational force distributions \$\mathbf{F}_A\$ and \$\mathbf{F}_B\$ per unit mass; see (3.2).

where \$\nabla\$ contracts with \$\mathbf{u}_g\$. This follows from multiplying (2.15) by \$\mathbf{k}\$ and using (2.7), (2.13) as well as \$\nabla \times \mathbf{F}' = 0\$ (cf. Andrews & McIntyre 1978 for a more general definition of \$\mathbf{p}\$, and the recent work of Bühler & Jacobson 2001 for details of a specific computation in shallow water). Unlike wave action, pseudomomentum can be created or destroyed without forcing or dissipation if the background flow is inhomogeneous as measured by non-vanishing \$\partial\Omega/\partial\mathbf{x}\$ hence \$\mathrm{d}\mathbf{k}/\mathrm{d}t\$. As is well known, components of \$\mathbf{p}\$ in translational-symmetry directions of the background state are conserved. However, all components of \$\mathbf{p}\$, whether conserved or not, play an important generic role in wave-mean interaction theory. This is important when carrying insights from shallow-water theory over to more realistic stratified models (Bretherton 1969; Bühler & McIntyre 1998). For reasons that emerge most plainly from a generalized Lagrangian-mean framework, it is \$\mathbf{p}\$ that is relevant to such generalizations, not the Stokes drift.

3. Recoil without vortex

To set the scene for what follows, we now consider the simple recoil scenario depicted in figure 1. There is no background velocity (\$\mathbf{U}=0\$) and hence the background layer depth \$H=1\$. Let \$x\$ and \$y\$ be Cartesian coordinates with \$x\$ pointing to the right in figure 1. A narrow beam of waves \$\{\mathbf{u}', h'\}\$ with constant wavenumber vector \$\mathbf{k}=(k, 0)\$ is emitted at \$x=-L\$ by the wave source on the left, travels across from left to right, and is then absorbed by a suitably tuned wave sink on the right, at \$x=+L\$. As indicated, both the emitting and the absorbing device experience mean \$O(a^2)\$ recoil forces in the \$x\$-direction denoted by \$\mathbf{R}_A\$ and \$\mathbf{R}_B\$. In any reasonable model we expect that

$$\mathbf{R}_A + \mathbf{R}_B = 0, \quad (3.1)$$

and this will now be shown on the assumption that the source and sink can be modelled by irrotational body-force distributions \$\mathbf{F}_A\$ and \$\mathbf{F}_B\$, respectively, defined so as to have exactly zero mean. For instance, a suitable form for \$\mathbf{F}_A\$ would be \$\mathbf{F}_A = \nabla\phi_A\$ with

$$\phi_A = a \operatorname{env}(x/l_E, y/l_E) \cos(k(x - c_0 t)), \quad (3.2)$$

where \$\operatorname{env}(\cdot)\$ is an order-unity smooth envelope function with envelope scale \$l_E\$ such that \$kl_E \gg 1\$ (see e.g. Bühler & McIntyre 1998 for a numerical implementation). Clearly, this \$\mathbf{F}_A\$ has zero mean (i.e. \$\mathbf{F}_A = \mathbf{F}'_A\$) and is precisely \$O(a)\$. It generates an essentially one-dimensional wavetrain travelling from left to right, i.e. the group velocity is \$\mathbf{u}_g(x, y) = (c_0, 0)\$ with corresponding rays given by \$y = \text{const}\$. For a steady wavetrain (2.15) means that

$$\nabla \cdot (HA \mathbf{u}_g) = 0 \quad (3.3)$$

outside the wave source and sink areas. In the present case (3.3) further reduces to $\partial A/\partial x = 0$, i.e.

$$A(x, y) = A_s(y) \quad (3.4)$$

if one denotes by $A_s(y)$ the profile of A just to the right of the wave source. As $\hat{\omega} = \text{const.}$ and $\mathbf{k} = \text{const.}$, the same statement is also true for E and \mathbf{p} .

Now, by momentum conservation (2.3) the mean recoil force \mathbf{R}_A is given by the integral of

$$-\bar{h}\overline{\mathbf{F}_A} = -\bar{h}\overline{\mathbf{F}_A} - \bar{h'}\overline{\mathbf{F}'_A} = -\bar{h'}\overline{\mathbf{F}'_A} \quad (3.5)$$

over the source area. Here the first term is zero by assumption because \mathbf{F}_A has zero mean, by virtue of (3.2). To $O(a^2)$, the second term can be evaluated using the solutions to the linear $O(a)$ equations (2.5). This shows that \mathbf{R}_A is a wave property, i.e. to leading order it can be computed on the basis of the linear solution alone. Comparison with (2.18) shows that $-\mathbf{R}_A$ is equal to the net flux of \mathbf{p} away from the source area:

$$\mathbf{R}_A = - \iint_{\text{source}} \bar{h'}\overline{\mathbf{F}'_A} dx dy = - \oint H\mathbf{p}(\mathbf{u}_g \cdot \hat{\mathbf{n}}) ds, \quad (3.6)$$

where $\hat{\mathbf{n}}$ is the outward-pointing unit normal vector. Thus one obtains the result that the source recoil is equal to minus the net rate of creation of \mathbf{p} by the source. This kind of result is typical for zero-mean irrotational wave sources, as illustrated for instance by idealized forms of toy boats propelled by a wavemaker at the rear (Longuet-Higgins 1977).

The same argument can be made for the wave sink modelled by a suitably tuned irrotational force $\mathbf{F}_B = \nabla\phi_B$. This then leads to the conclusion that the sink recoil \mathbf{R}_B is equal to the net destruction rate of \mathbf{p} per unit time; hence one arrives at (3.1).

One can note in passing that this argument relied crucially on $\overline{\mathbf{F}_A} = \overline{\mathbf{F}_B} = 0$ at $O(a^2)$. For instance, one might be tempted to model the wave sink by Rayleigh friction such that $\mathbf{F}_B \propto -\mathbf{u}$, which preserves the irrotationality of \mathbf{u} . However, one would then have $\overline{\mathbf{F}_B} \propto -\overline{\mathbf{u}}$, which need not be zero at $O(a^2)$. As $\overline{\mathbf{u}}$ cannot be deduced from the linear solution alone, this would leave \mathbf{R}_B undetermined at this stage. This illustrates the care that has to be taken when implementing (say, in a numerical simulation) zero-mean irrotational forces at $O(a^2)$ or higher.

3.1. Mean-flow response

The averaged continuity equation (2.1) is

$$\frac{\partial \bar{h}}{\partial t} + \nabla \cdot (\bar{h}\overline{\mathbf{u}} + \bar{h'}\overline{\mathbf{u}'}) = 0, \quad (3.7)$$

which in the present case reduces to

$$\nabla \cdot \overline{\mathbf{u}} = -\nabla \cdot \mathbf{p} = -k \frac{\partial A}{\partial x} \quad (3.8)$$

at $O(a^2)$. Comparison with (3.4) shows that this right-hand side is non-zero only in the wave source and sink regions. Specifically, the apparent mass source is negative at the wave source and positive at the wave sink. Now, the flow is by assumption irrotational throughout (having started from rest and being driven by irrotational forces); hence

$$\nabla \times \mathbf{u} = 0 \quad \text{and} \quad \nabla \times \overline{\mathbf{u}} = 0. \quad (3.9)$$

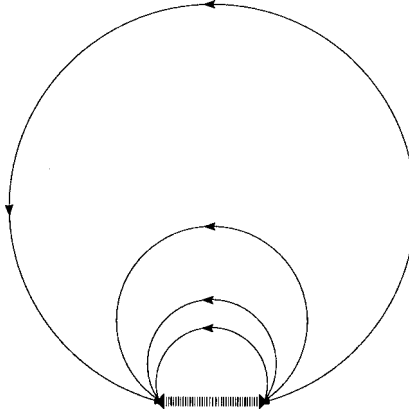


FIGURE 2. Streamlines of the $O(a^2)$ irrotational mean flow \bar{u} described by (3.10) when the wave source and sink are arranged as in figure 1. To save space, only half of the mirror-symmetric source–sink flow is depicted. At large distances $r \gg L$, the velocity field takes dipole form, decaying as $1/r^2$. In a Lagrangian-mean picture, the flow would be non-divergent and would continue along the wavetrain. Because the wave field is steady there is no ‘divergence effect’.

Together with suitable boundary conditions, (3.8)–(3.9) determine \bar{u} completely at $O(a^2)$ in terms of the known $O(a)$ wave fields feeding into the right-hand side of (3.8). Specifically,

$$\bar{u}(x, y) = \frac{1}{2\pi} \iint \frac{(x - x', y - y')}{(x - x')^2 + (y - y')^2} \left[-k \frac{\partial A}{\partial x}(x', y') \right] dx' dy'. \quad (3.10)$$

Figure 2 shows some streamlines of \bar{u} . To save space, only half of the mirror-symmetric source–sink flow is depicted. At distances r from the wavetrain that are large in comparison with the source–sink distance $2L$, the return flow is dipolar and decays as $1/r^2$. The implied particle trajectories (i.e. the integral curves of the leading-order Lagrangian-mean velocity $\bar{u} + \bar{h}'\bar{u}'$) in this case resemble Feynman’s ‘children on a slide’ image of the flow in and around an acoustic wavepacket (§ 11.5 in Feynman 1998).

Finally, the depth disturbance at $O(a^2)$ can be easily calculated from Bernoulli’s theorem for potential flows. As the wave source and sink are due to irrotational forces with zero-mean potential, they make no contribution to the averaged Bernoulli theorem

$$\frac{\bar{u} \cdot \bar{u}}{2} + \frac{\bar{u}' \cdot \bar{u}'}{2} + \frac{c_0^2}{\gamma - 1} \bar{h}^{\gamma-1} = \frac{c_0^2}{\gamma - 1}, \quad (3.11)$$

which after expansion in powers of wave amplitude and using (2.16) yields

$$\bar{h} = 1 - \frac{d(\ln c)}{d(\ln H)} \frac{E}{c_0^2} = 1 - \frac{\gamma - 1}{2} \frac{E}{c_0^2} \quad (3.12)$$

to $O(a^2)$. This is the well known hard-spring or mean density dilatation effect (for $\gamma > 1$) inside a wavetrain (Brillouin 1925). It can be shown that (3.12) corresponds to uniform mean pressure, $\nabla \bar{p} = 0$ in (2.3) , throughout the domain.

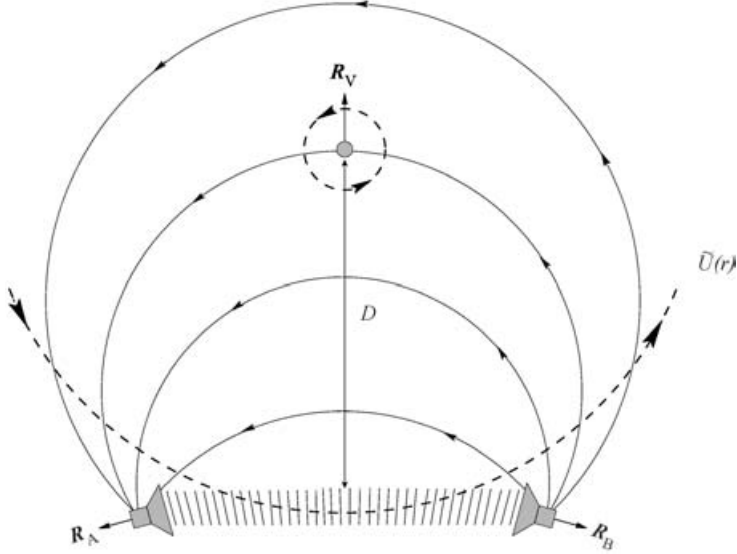


FIGURE 3. A background vortex with circulation $\Gamma > 0$ has been added a distance D to the left of the wavetrain, where it is exposed to the large-scale return flow shown in figure 2 (solid curves). The background velocity of the vortex (dashed curves) pushes the wave rays toward decreasing y at the source and pulls them toward increasing y at the sink. To keep $y = \text{const.}$ along the rays (Landau & Lifshitz 1987), the phase lines have to tilt slightly as indicated; see (4.11). This leads to tilted recoil forces and to a net vortex recoil \mathbf{R}_V ; see (4.1)ff. and (4.25).

4. Remote recoil with vortex

Consider now the situation depicted in figure 3. An $O(1)$ background vortex has been placed in the region of weak return flow far away from the wavetrain. This has two effects. First, the wavetrain is modified, as the waves are now refracted by the non-uniform background flow due to the vortex. Second, the vortex can be expected to migrate slowly to the left because of advection by the $O(a^2)$ return flow — as if the waves were absent but a transverse force \mathbf{R}_V in the y -direction were being exerted on the vortex core. It will be shown that these two effects are intimately linked.

To simplify matters we assume at first that an artificial $O(a^2)$ holding force $\mathbf{F}_H(\mathbf{x})$ per unit mass acts on the vortex to cancel its advection, allowing the mean flow to remain steady. The vortex-core recoil \mathbf{R}_V can then be equated to minus the resultant of \mathbf{F}_H :

$$\mathbf{R}_V = - \iint h \mathbf{F}_H \, dx \, dy. \quad (4.1)$$

In order for the flow to be steady, we must have from (2.3) that

$$h \mathbf{F}_H = \nabla \cdot (h u \mathbf{u} + p \mathbf{I}), \quad (4.2)$$

where \mathbf{I} is the unit tensor, and hence from (4.1) that

$$\mathbf{R}_V = - \oint (h u \mathbf{u} \cdot \hat{\mathbf{n}} + p \hat{\mathbf{n}}) \, ds, \quad (4.3)$$

where the line integral encloses the vortex core, outside which \mathbf{F}_H is assumed to vanish, and where ds and $\hat{\mathbf{n}}$ are the line element and outward normal. The distribution of \mathbf{F}_H inside the vortex core is of course not unique. But we shall be concerned only with the resultant as defined by (4.1) and (4.3), which depends only on conditions outside the vortex core.

4.1. Background vortex flow

Let the origin of the coordinate system coincide with the centre of the vortex and let D be the minimum distance from vortex to wavetrain. This means that the wave source is centred at $(-L, -D)$ and the wave sink at $(+L, -D)$. The vortex is axisymmetric with circumferential velocity $\tilde{U}(r)$ and depth field $H(r)$, with $r^2 = x^2 + y^2$. The detailed structure of the vortex core is unimportant, provided that the background vorticity is confined within a core of radius b so that for $r > b$ the velocity profile is $\tilde{U}(r) = \Gamma/(2\pi r)$, where $\Gamma > 0$ is the circulation. The radius $b \ll D$, and the line integral in (4.3) can be taken around $r = b$. The $O(1)$ velocity and depth field in cyclostrophic balance are

$$\mathbf{U} = (U, V) = \frac{\Gamma}{2\pi} \left(\frac{-y}{r^2}, \frac{+x}{r^2} \right), \quad H^{\gamma-1} = 1 - \frac{\gamma-1}{2} \frac{\tilde{U}^2}{c_0^2} \quad (4.4)$$

for $r > b$.

We will from now on assume that the vortex is weak in the sense that \tilde{U}/c_0 is a small number everywhere, i.e. the vortex Froude (or Mach) number is small. A convenient dimensionless small parameter for this assumption (for fixed D) is

$$\epsilon = \frac{|\Gamma|}{2\pi c_0 D} \ll 1. \quad (4.5)$$

There are now two small parameters: a for the wave amplitude and ϵ for the vortex amplitude. It is necessary that $\epsilon \gg a$ such that the $O(\epsilon)$ background vortex can still be treated as a background flow that is large, $O(1)$, in comparison with the $O(a)$ linear waves. This also allows us to treat terms $O(a^n \epsilon^m)$ (where n, m are non-negative integers) as much bigger than $O(a^{n+1})$ terms, which will be useful below. Only terms up to $O(a^n \epsilon^2)$ will be considered, for instance we will approximate (4.4) by

$$H = 1 - \frac{\tilde{U}^2}{2c_0^2}. \quad (4.6)$$

One can note in passing that, presumably, a distinguished limit such as $a \propto \epsilon^3$ could be used to make rigorous the formal asymptotics presented here.

4.2. Linear waves

For non-uniform H the local wave speed

$$c = c_0 \sqrt{H^{\gamma-1}} = c_0 \left(1 - \frac{\gamma-1}{4} \frac{\tilde{U}^2}{c_0^2} \right) \quad (4.7)$$

to $O(\epsilon^2)$. To the same order the absolute frequency of the waves is given by

$$\omega = \hat{\omega} + \mathbf{U} \cdot \mathbf{k} = c_0 \kappa + \mathbf{U} \cdot \mathbf{k} - \frac{\gamma-1}{4} \frac{\tilde{U}^2}{c_0} \kappa, \quad (4.8)$$

where terms have been ordered in powers of ϵ . The corresponding absolute group velocity is

$$\mathbf{u}_g = c \frac{\mathbf{k}}{\kappa} + \mathbf{U} = c_0 \frac{\mathbf{k}}{\kappa} + \mathbf{U} - \frac{\gamma - 1}{4} \frac{\tilde{U}^2}{c_0} \frac{\mathbf{k}}{\kappa}. \quad (4.9)$$

In addition to the previously noted ray-invariance of the absolute frequency ω (due to the steadiness of the background flow) there is also a second invariant due to the axisymmetry of this particular background flow:

$$\omega = \text{const.} \quad \text{and} \quad lx - ky = \text{const.} \quad (4.10)$$

This second invariant is equal to the angular pseudomomentum per unit wave action; it will not be important here. Now, even truncated to $O(\epsilon^2)$ the ray-tracing equations are difficult to solve analytically. Also, at $O(\epsilon^2)$ the value of γ matters in (4.9), which means that at this order the wave field depends on the nonlinear details of the fluid compressibility. On the other hand, it will turn out that knowing the wave field to $O(\epsilon^n)$ is sufficient to determine the recoil force at $O(\epsilon^{n+1})$. If the ray-tracing equations can be integrated at $O(\epsilon)$ then this will allow us to compute the recoil force up to $O(\epsilon^2)$. This is pursued now. We assume that ω has the same value on all rays, which is consistent with a normal-mode approach. That is, $\omega = c_0 k_0$ everywhere with a suitable constant $k_0 > 0$ such that $\mathbf{k} = (k_0, 0) + O(\epsilon)$.

We now make use of the classical result that non-dispersive wave rays through an irrotational background flow are straight lines to $O(\epsilon)$, i.e. to first order in Froude (or Mach) number (e.g. Landau & Lifshitz 1987, p. 261; the result readily generalizes to isotropically dispersive waves with large intrinsic group velocities relative to the background flow, see e.g. Dysthe 2001). This remarkable result (which can be derived from Fermat's principle of least time) says that whilst \mathbf{k} and hence the intrinsic group velocity are constantly changed by refraction due to \mathbf{U} , the absolute group velocity \mathbf{u}_g always points in the same direction. Referring to figure 3 this means that if, as indicated, the wavemaker on the left is slightly tilted toward the vortex in order to make $v_g = 0$ at the source, then v_g will continue to be zero along the ray, i.e. the ray is simply $y = \text{const.}$ From this argument and (4.9) it follows that, to $O(\epsilon)$,

$$v_g = 0, \quad \Rightarrow \quad l = -k_0 \frac{V}{c_0}, \quad (4.11)$$

with l taking opposite signs at the source and sink. This corresponds to the pushing or pulling action of the background flow at these locations. Now, using the fact that $\nabla \times \mathbf{k} = 0$ by definition, we can obtain k from (4.11) by integration, recalling that $\nabla \times \mathbf{U} = 0$ from (4.4), to get

$$k = k_0 - k_0 \frac{U}{c_0}, \quad \text{that is} \quad \mathbf{k} = (k_0, 0) - k_0 \frac{\mathbf{U}}{c_0}. \quad (4.12)$$

It is straightforward to check that this solution satisfies all the ray-tracing equations to $O(\epsilon)$; and one can note in passing that the angular-pseudomomentum invariant (4.10) differs from ray to ray, i.e. it depends on y , unlike the globally constant ω . Also, whilst $\nabla \times \mathbf{k} = 0$ by definition, $\nabla \cdot \mathbf{k} = 0$ also holds in this special case. Finally, it can easily be verified that the rays connecting the source and sink remain straight lines to $O(\epsilon)$ even in the limit as $L \rightarrow \infty$ for fixed ϵ , a fact to be made use of in §5.

The wave-action profile $A(x, y)$ inside the wavetrain is computed from (3.3) using the group velocity $\mathbf{u}_g = (c_0 + U, 0)$. The result is

$$A(x, y) = A_s(y) \frac{c_0 + U(-L, y)}{c_0 + U(x, y)} = A_s(y) \left(1 + \frac{\Gamma}{2\pi c_0} \frac{y(L^2 - x^2)}{(x^2 + y^2)(L^2 + y^2)} \right) \quad (4.13)$$

to $O(\epsilon)$; recall that $\Gamma/2\pi c_0 = \epsilon D$. As before, $A_s(y)$ is the value of A just to the right of the source. As $y \approx -D$ in the wavetrain, A has a minimum at closest approach to the vortex. Physically this is because $u_g = c_0 + U$ is greatest there, diluting the wave action.

4.3. Mean-flow response

The $O(a^2)$ mean-flow response in the presence of a vortex is significantly more complicated than before; see especially §5 below, where the $O(\epsilon)$ term in (4.13) will be essential. Furthermore, the need to distinguish clearly between contributions at various powers of a and ϵ makes it convenient to introduce a special notation as follows. A single subscript denotes the total contribution to a quantity at the corresponding power of a . A second subscript, if present, denotes the contribution at the corresponding power of ϵ . Thus, for instance,

$$\bar{\mathbf{u}}_2 = \bar{\mathbf{u}}_{20} + \bar{\mathbf{u}}_{21} + \bar{\mathbf{u}}_{22} + \dots, \quad (4.14)$$

where the left-hand side is the total mean-flow response at $O(a^2)$ and the right-hand side shows the contributions at $O(a^2\epsilon^0)$, $O(a^2\epsilon^1)$, etc. By assumption $1 \gg \epsilon \gg a$ such that these terms are formally much larger than $\bar{\mathbf{u}}_3$. In this notation the $O(a^2)$ mean-flow response terms without a vortex, i.e. $\bar{\mathbf{u}}$ in (3.10) and $\bar{h} - 1$ in (3.12), become $\bar{\mathbf{u}}_{20}$ and \bar{h}_{20} , respectively.

As noted before, the mean flow is held steady by the action of a suitable vortex holding-force distribution $\mathbf{F}_H(\mathbf{x})$, which is non-zero only inside the vortex core; thus $\mathbf{F}_H = 0$ for $r > b$. Crucially, unlike the body forces at the wave source and sink, the holding force \mathbf{F}_H must be allowed to have non-zero curl. Consider now the problem of appropriately choosing this \mathbf{F}_H at leading order, which is $O(a^2\epsilon)$. At this order the steady mean-momentum equation near the vortex is

$$(\mathbf{U} \cdot \nabla) \bar{\mathbf{u}}_{20} + (\bar{\mathbf{u}}_{20} \cdot \nabla) \mathbf{U} + c_0^2 \nabla \bar{h}_{21} = \mathbf{F}_H. \quad (4.15)$$

There are no disturbance correlation terms, because there are no waves near the vortex. With the help of a vector identity the first two terms can be rewritten as

$$\nabla(\mathbf{U} \cdot \bar{\mathbf{u}}_{20}) + (\nabla \times \mathbf{U}) \times \bar{\mathbf{u}}_{20} + (\nabla \times \bar{\mathbf{u}}_{20}) \times \mathbf{U}, \quad (4.16)$$

which because of $\nabla \times \bar{\mathbf{u}}_{20} = 0$ yields

$$\nabla(\mathbf{U} \cdot \bar{\mathbf{u}}_{20} + c_0^2 \bar{h}_{21}) = \mathbf{F}_H - (\nabla \times \mathbf{U}) \times \bar{\mathbf{u}}_{20}. \quad (4.17)$$

We may use the latitude of choice permitted by (4.1)–(4.3) to make \mathbf{F}_H as simple as possible. We choose

$$\mathbf{F}_H = (\nabla \times \mathbf{U}) \times \bar{\mathbf{u}}_{20}. \quad (4.18)$$

Then, to satisfy (4.17) and to match to the solution outside the vortex core we must take

$$c_0^2 \bar{h}_{21} = -\mathbf{U} \cdot \bar{\mathbf{u}}_{20} \quad (4.19)$$

inside the vortex core, as well as just outside. The solution just outside must conform to (3.11) because Bernoulli's theorem for potential flow holds there. Because there are

no waves there, (3.11) at $O(a^2\epsilon)$ leads again to (4.19). We may now evaluate (4.3) on the circle $r=b$, correct to $O(a^2\epsilon)$, and recalling (4.6) (permitting $H=1$ here), as

$$\mathbf{R}_V = - \int_0^{2\pi} (c_0^2 \bar{h}_{21} \mathbf{I} + \mathbf{U} \bar{\mathbf{u}}_{20} + \bar{\mathbf{u}}_{20} \mathbf{U})|_{r=b} \cdot \hat{\mathbf{n}} b d\theta, \quad (4.20)$$

where θ is the polar angle and where the outward normal $\hat{\mathbf{n}}$ now has Cartesian components $(\cos\theta, \sin\theta)$. The last term in the integrand is zero, because $\mathbf{U} \cdot \hat{\mathbf{n}} = 0$, and \bar{h}_{21} can be eliminated from the first term via (4.19) to give

$$\mathbf{R}_V = - \int_0^{2\pi} (-\mathbf{U} \cdot \bar{\mathbf{u}}_{20} \mathbf{I} + \mathbf{U} \bar{\mathbf{u}}_{20})|_{r=b} \cdot \hat{\mathbf{n}} b d\theta. \quad (4.21)$$

This integral can be evaluated without ambiguity; indeed, since $\bar{\mathbf{u}}_{20}$ is slowly varying near the vortex one can approximate it in (4.21) by a constant equal to its value at the vortex centre ($x=0, y=0$). Then, noting that the Cartesian components of \mathbf{U} at $r=b$ are $(-\sin\theta, \cos\theta)\Gamma/(2b\pi)$, we can easily evaluate the integral. Both terms make equal contributions to the net result, which is

$$\mathbf{R}_V = -\Gamma \hat{\mathbf{z}} \times \bar{\mathbf{u}}_{20}(0, 0) = \Gamma |\bar{\mathbf{u}}_{20}| \hat{\mathbf{y}}, \quad (4.22)$$

where $\hat{\mathbf{y}}$ is the unit vector in the y -direction and $|\bar{\mathbf{u}}_{20}|$ is evaluated at the vortex centre. This shows that the effective recoil force \mathbf{R}_V is given by a Magnus force expression. As an aside one can note that the above computation can be repeated with a solid cylinder replacing the vortex. The changed boundary condition at the cylinder boundary modifies the flow such that the classical Magnus force computation applies, with the recoil force now equal to the Magnus force.

Now, the value for $\bar{\mathbf{u}}_{20}(0, 0)$ is given by (3.10) at the origin, which by symmetry has zero y -component and an x -component that is twice that due to the source alone. The x -component can be simplified by approximating the slowly varying pre-factor in the integrand of (3.10) by its value at the source, i.e. at $(x', y')=(-L, -D)$. With $(x, y)=(0, 0)$ this yields

$$\bar{\mathbf{u}}_{20}(0, 0) = -\frac{2}{2\pi} \iint_{\text{source}} \frac{(L, 0)}{L^2 + D^2} k_0 \frac{\partial A}{\partial x}(x', y') dx' dy' = -\frac{k_0}{\pi} \frac{(L, 0)}{L^2 + D^2} \int_{-\infty}^{+\infty} A_s(y') dy'. \quad (4.23)$$

The vortex recoil force is then

$$\mathbf{R}_V = \hat{\mathbf{y}} \frac{k_0 \Gamma}{\pi} \frac{L}{L^2 + D^2} \int_{-\infty}^{+\infty} A_s(y') dy'. \quad (4.24)$$

This expression can be cross-checked by evaluating the y -components of the source and sink recoil forces in (3.6) to $O(a^2\epsilon)$. Using $H=1$ again, the wavenumber l from (4.11), $\mathbf{u}_g = c_0 \hat{\mathbf{x}}$ and the fact that source and sink have the same recoil y -component, one readily verifies that

$$\mathbf{R}_A + \mathbf{R}_B + \mathbf{R}_V = 0. \quad (4.25)$$

This confirms that the vortex holding force was indeed necessary, in order to keep the net momentum budget balanced for steady-state conditions.

4.4. Vortex response without holding force

If the vortex holding force is removed then the mean flow is not steady any more. The unsteady mean flow that ensues can be understood if one imagines the holding

force to lapse just for a small time interval Δt , after which the force is then switched on again, at time $t = 0$, say, and the flow becomes steady again. Within the present perturbation regime, this is equivalent to the linear response of a shallow-water vortex without waves to the application of a transient force $-\mathbf{F}_H$ per unit mass to the vortex core, with net impulse $\Delta t \mathbf{R}_V$.

Clearly, there will be a net input of y -momentum into the fluid equal to $\Delta t \mathbf{R}_V$. At the same time, in response to $\nabla \times (-\mathbf{F}_H)$, the vortex will move a distance $\Delta x = \bar{u}_{20} \Delta t$, to the left in figure 3, i.e. in the $-x$ -direction. Now, as the flow again settles down to a steady state, this will change the amount of y -momentum contained in a large fixed circle centred at the original vortex location, by an amount asymptotically equal to just half of $\Delta t \mathbf{R}_V$. (The specification of the control volume is crucial because the total momentum integral for a single vortex is only conditionally convergent, as is the total momentum integral for the dipolar difference field, defined as \mathbf{U} for the displaced vortex minus \mathbf{U} for the undisplaced vortex.) The other half of the momentum $\Delta t \mathbf{R}_V$ resides in the wavefront of an $O(a^2)$ mean dipolar gravity-wave pulse, propagating radially outward with speed c_0 , and which adjusts the far-field vortex flow to the changed vortex core location. This is the far-field recoil alluded to in the introduction.

In other words, only half of the recoil momentum will be found in the balanced vortical flow at large times; the other half will be found in the velocity field of the $O(a^2)$ mean gravity-wave pulse. At any moment in time t , the corresponding wavefront will be near $r = c_0 t$. This is analogous to classical results about the impulsive forcing of incompressible flow, with the difference that there the recoil wave reaches spatial infinity instantaneously.

Finally, one can check that the hydrodynamical impulse of the dipolar difference field (e.g. Lamb 1932) is asymptotically $-\Delta x \Gamma \hat{\mathbf{y}} = \Delta t \mathbf{R}_V$. This is just equal to the recoil momentum, as is the case for incompressible flow.

5. Source and sink at infinity

As shown by (4.4) and (4.24), the magnitude of the vortex recoil force \mathbf{R}_V at $O(a^2\epsilon)$ is proportional to $|\mathbf{U}|$ at the wave source or sink, and goes to zero like $1/L$ when $L \rightarrow \infty$. This again can be cross-checked by re-evaluating (3.6) to $O(a^2\epsilon)$. As $L \rightarrow \infty$, one obtains a classical scattering problem in which waves approach from and recede to spatial infinity. Leaving aside questions of uniformity, related to the diffractive Rayleigh length, etc., we see that there is an interesting evolution of \mathbf{k} along the wave ray. The y -component l is still governed by (4.11), implying that the phase tilts seen in figure 3 still occur and also that $l \rightarrow 0$ as $x \rightarrow \pm\infty$. Thus \mathbf{k} starts parallel to the x -axis at $x = -\infty$, swings toward the vortex as the waves approach then away as they recede, before again becoming parallel to the x -axis at $x = +\infty$. Most importantly, this implies that $\mathbf{R}_V \rightarrow 0$ as $L \rightarrow \infty$.

To obtain a non-zero answer in this scattering limit $L \rightarrow \infty$ one has to go to the next order in ϵ , more precisely, to $O(a^2\epsilon^2)$. At this order, the outgoing and incoming l values differ by a finite amount proportional to the scattering angle of the wave. From the recoil force to $O(a^2\epsilon^2)$ this scattering angle could be computed directly from (3.6) and (4.25). As the $O(a^2\epsilon^2)$ recoil force can be computed using only the $O(a\epsilon)$ wave field and $O(a^2\epsilon)$ mean-flow response, this means that the scattering angle can be explicitly found in this way, i.e. without ever solving the linear ray-tracing equations at $O(\epsilon^2)$.

5.1. Recoil force

The main task is to compute $\bar{\mathbf{u}}_{21}$. This is carried out for the steady state subject to the holding force (4.18), with $\bar{\mathbf{u}}_{21}$ in place of $\bar{\mathbf{u}}_{20}$ since $\bar{\mathbf{u}}_{20}$ is now zero. As before, $\nabla \times \bar{\mathbf{u}}_{21} = 0$, because outside the vortex core the flow is strictly irrotational, and inside the vortex core the holding force keeps the vorticity strictly steady and unchanged. Furthermore, it is readily verified that the near-vortex momentum balance (4.15) and the Magnus formula (4.22) also apply at the next order in ϵ , i.e. with $\bar{\mathbf{u}}_{20}$ replaced by $\bar{\mathbf{u}}_{21}$ and \bar{h}_{21} by \bar{h}_{22} . There is an additional term proportional to $(H - 1)\bar{h}_{20}$; but $\bar{h}_{20} = 0$ at the vortex. This extension to the next order in ϵ also applies to the Bernoulli equation that provides the boundary condition for \bar{h}_{22} . Therefore, the only new equation comes from the steady mean continuity equation (3.7), which at $O(a^2\epsilon)$ is

$$\nabla \cdot \bar{\mathbf{u}}_{21} = -\nabla \cdot \mathbf{p}_{21} - \nabla \cdot (\bar{h}_{20} \mathbf{U}). \quad (5.1)$$

Here \mathbf{p}_{21} is the $O(a^2\epsilon)$ part of $\mathbf{p} = \mathbf{k}A$, which can be read off from (4.12) and (4.13) in the limit $L \rightarrow \infty$; and \bar{h}_{20} is equal to the last term in (3.12). Evaluating the right-hand side of (5.1) is made easier by recalling that $\nabla \cdot \mathbf{U} = 0$ and $\nabla \cdot \mathbf{k} = 0$. The result is

$$\nabla \cdot \bar{\mathbf{u}}_{21} = \frac{k_0 \Gamma}{2\pi c_0} \left\{ \frac{2xy}{r^4} A_s(y) + \frac{\gamma + 1}{2} \frac{x}{r^2} \frac{dA_s}{dy}(y) \right\}. \quad (5.2)$$

Two contributions in dA_s/dy have been combined into one term here.

Applying the inversion formula analogous to (3.10) to (5.2) with $\nabla \times \bar{\mathbf{u}}_{21} = 0$ gives

$$\bar{\mathbf{u}}_{21}(0, 0)$$

$$= -\frac{k_0 \Gamma}{(2\pi)^2 c_0} \iint \frac{(x', y')}{x'^2 + y'^2} \left\{ \frac{2x'y'}{(x'^2 + y'^2)^2} A_s(y') + \frac{\gamma + 1}{2} \frac{x'}{x'^2 + y'^2} \frac{dA_s}{dy}(y') \right\} dx' dy' \quad (5.3)$$

for the velocity at the vortex core, where x' now ranges between $\pm\infty$ as well as y' . Again, the y -component of this integral vanishes by symmetry. For the x -component the terms in A_s and dA_s/dy are considered separately. The x' -integral for the former can be evaluated exactly, and in the remaining y' -integral one can use $y' \approx -D$ in the slowly varying pre-factor. The result is

$$\frac{k_0 \Gamma \operatorname{sgn}(D)}{16\pi c_0 D^2} \int_{-\infty}^{+\infty} A_s(y') dy', \quad (5.4)$$

where $\operatorname{sgn}(D)$ is ± 1 according to the sign of D , the upper sign corresponding to waves passing to the right of the vortex as before. The term in dA_s/dy is treated in just the same way, after converting it to a term in $A_s(y')$ using integration by parts in y' . This is straightforward because A_s is zero outside the wavetrain; there are no boundary terms. The result, for the term in dA_s/dy , is

$$\frac{k_0 \Gamma (\gamma + 1) \operatorname{sgn}(D)}{16\pi c_0 D^2} \int_{-\infty}^{+\infty} A_s(y') dy'. \quad (5.5)$$

Adding the two results, we have finally

$$\bar{\mathbf{u}}_{21}(0, 0) = \hat{\mathbf{x}} \frac{k_0 \Gamma (\gamma + 2) \operatorname{sgn}(D)}{16\pi c_0 D^2} \int_{-\infty}^{+\infty} A_s(y') dy'. \quad (5.6)$$

As noted before, (4.15) and the Magnus formula (4.22) are unchanged in appearance

at the next order in ϵ , and hence the recoil force at $O(a^2\epsilon^2)$ for scattering waves is given by

$$\mathbf{R}_V = -\Gamma \hat{\mathbf{z}} \times \bar{\mathbf{u}}_{21}(0, 0) = -\hat{\mathbf{y}} \frac{k_0 \Gamma^2 (\gamma + 2) \operatorname{sgn}(D)}{16\pi c_0 D^2} \int_{-\infty}^{+\infty} A_s(y') dy'. \quad (5.7)$$

Being quadratic in Γ , this force is the same regardless of the sign of the vortex circulation. This is related to the approximate mirror symmetry of figure 4 below. However, \mathbf{R}_V does change sign according to whether the waves pass to the right of the vortex ($D > 0$) or to the left of it ($D < 0$).

Notice that, for $\gamma > -2$, (5.6) implies that $\bar{\mathbf{u}}_{21}(0, 0)$ at the vortex core is in the positive x -direction. Because of the bending of the wavetrain and the retreat of source and sink to $x = \pm\infty$, $\bar{\mathbf{u}}_2(0, 0)$ and \mathbf{R}_V have both reversed their directions relative to those in figure 3.

5.2. Global momentum budget and scattering angle

From the recoil force at $O(a^2\epsilon^2)$ one can now compute the scattering angle of the waves. In fact, it appears that this can be done in general at $O(a^2)$, i.e. without restriction to small ϵ . The result now to be obtained is based on a global momentum budget argument, which, as will be shown, establishes an equality between $-\mathbf{R}_V$ and the total or global rate of change of pseudomomentum. The analysis is not completely straightforward, and will therefore be demonstrated in some detail. The starting point is again the flux form (4.2) of the exact momentum equation, but now integrated over a large circular area of radius r , say. After averaging (with the wave source and sink still at $x = \pm\infty$), this gives

$$\mathbf{R}_V = - \iint \overline{h \mathbf{F}_H} dx dy = - \int_0^{2\pi} (\overline{h u u} + \overline{p I}) \cdot \hat{\mathbf{n}} r d\theta, \quad (5.8)$$

with pressure $p = c_0^2 h^\gamma / \gamma$ and vortex-holding force \mathbf{F}_H . At $O(a^2)$ the right-hand side becomes

$$- \int_0^{2\pi} (\overline{h}_2 \mathbf{U} \mathbf{U} + H \overline{\mathbf{u}}_2 \mathbf{U} + \overline{h'_1 \mathbf{u}'_1} \mathbf{U} + \mathbf{U} \overline{h'_1 \mathbf{u}'_1} + H \mathbf{U} \overline{\mathbf{u}}_2 + H \overline{\mathbf{u}'_1 \mathbf{u}'_1} + \overline{p}_2 \mathbf{I}) \cdot \hat{\mathbf{n}} r d\theta \quad (5.9)$$

and this will be investigated in the limit $r \rightarrow \infty$. Now, the first three terms are trivially zero because $\mathbf{U} \cdot \hat{\mathbf{n}} = 0$. The fourth term contains a factor equal to the pseudomomentum density, which is non-zero over a fixed arclength $r d\theta$ as $r \rightarrow \infty$. As $\mathbf{U} \propto 1/r$, this means that this term integrates to something of order at most $O(1/r)$, which goes to zero as $r \rightarrow \infty$. The narrow-wavetrain assumption is used here. The fifth term requires more care. Writing $\overline{\mathbf{u}}_2 = \nabla \overline{\phi}_2$, since $\nabla \times \overline{\mathbf{u}}_2 = 0$, we see that the fifth term becomes

$$- \int_0^{2\pi} H \mathbf{U} (\nabla \overline{\phi}_2 \cdot \hat{\mathbf{n}}) r d\theta = -H(r) \frac{\Gamma}{2\pi} \int_0^{2\pi} (-\sin \theta, \cos \theta) \frac{\partial \overline{\phi}_2}{\partial r} d\theta. \quad (5.10)$$

Because $H \rightarrow 1$, (5.10) makes clear that this fifth term integrates to something proportional to the first Fourier mode of $\partial \overline{\phi}_2 / \partial r$. In other words, if $\overline{\phi}_2$ is written as a sum of Fourier modes $a_n(r) \exp(in\theta)$ with integer n , then (5.10) is proportional to $|da_1(r)/dr|$.

Now, the steady mean continuity equation (3.7) at $O(a^2)$ yields

$$\nabla \cdot (H\bar{\mathbf{u}}_2 + H\mathbf{p} + U\bar{h}_2) = 0, \quad (5.11)$$

$$\Rightarrow \nabla^2 \bar{\phi}_2 + \frac{1}{H} \frac{dH}{dr} \frac{\partial \bar{\phi}_2}{\partial r} = -\frac{1}{H} \nabla \cdot (H\mathbf{p}) - \frac{U}{H} \cdot \nabla \bar{h}_2, \quad (5.12)$$

$$\Rightarrow \nabla^2 \bar{\phi}_2 \approx -\nabla \cdot \mathbf{p} - \mathbf{U} \cdot \nabla \bar{h}_2, \quad (5.13)$$

where the last line holds for large r with error $O(a^2r^{-2})$ because of cyclostrophic balance, (4.4). The free-space Green's function for the first Fourier mode of the Poisson equation decays as $1/r$, i.e. dipole behaviour, which means that difficulties can come only from the behaviour of the source terms in (5.11)–(5.13) for large r . Specifically, if the first-mode or dipolar part of the source terms on the right of the Poisson equation decays as $1/r^m$ at large distances then $a_1(r)$ satisfies

$$\frac{1}{r} \frac{d}{dr} \left(r \frac{da_1}{dr} \right) - \frac{1}{r^2} a_1 = \frac{1}{r^m}. \quad (5.14)$$

The solution is $a_1 \propto r^{2-m}$, which means that $|da_1(r)/dr|$ and therefore (5.10) will go to zero as $r \rightarrow \infty$ provided that $m > 1$. With this result in hand, it is possible to show from (2.18) and (3.11) that the first-mode or dipolar part of the source terms in (5.13) is bounded by $O(a^2r^{-2})$. Therefore we have at least $m=2$, which satisfies the decay condition $m > 1$ and finally proves that the contribution of the fifth term in (5.9) will also be negligible as $r \rightarrow \infty$.

For the sixth term it is straightforward to show that $H\bar{\mathbf{u}}'_1 \cdot \hat{\mathbf{n}}$ is equal to $H\mathbf{p}\mathbf{u}_g \cdot \hat{\mathbf{n}}$. Hence this term represents the pseudomomentum flux across the large circle $r=\text{constant}$. Like the fourth term, this sixth term is non-zero over a fixed arclength $r d\theta$ as $r \rightarrow \infty$. However, it is now multiplied by the non-decaying H . This term will therefore make a finite contribution as $r \rightarrow \infty$, which will be considered in detail below. Finally, the pressure term is

$$\bar{p}_2 = \frac{c_0^2}{\gamma} \bar{h}^\gamma \Big|_2 = c_0^2 H^{\gamma-1} \left(\bar{h}_2 + \frac{\gamma-1}{2} \frac{\overline{(h'_1)^2}}{H} \right). \quad (5.15)$$

This can be linked to the mean Bernoulli theorem at $O(a^2)$, which is

$$\mathbf{U} \cdot \bar{\mathbf{u}}_2 + \frac{1}{2} \bar{\mathbf{u}}'_1 \cdot \bar{\mathbf{u}}'_1 = -\frac{c_0^2}{\gamma-1} \bar{h}^{\gamma-1} \Big|_2 = -c_0^2 H^{\gamma-2} \left(\bar{h}_2 + \frac{\gamma-2}{2} \frac{\overline{(h'_1)^2}}{H} \right). \quad (5.16)$$

Combining (5.15) and (5.16) and rearranging leads to

$$\mathbf{U} \cdot \bar{\mathbf{u}}_2 + \frac{1}{H} \bar{p}_2 + \frac{1}{2} \bar{\mathbf{u}}'_1 \cdot \bar{\mathbf{u}}'_1 - \frac{c_0^2}{2} H^{\gamma-3} \overline{(h'_1)^2} = 0. \quad (5.17)$$

However, the last two terms are equal by the equipartition of wave energy noted in (2.16). This means that finally

$$\bar{p}_2 = -H \mathbf{U} \cdot \bar{\mathbf{u}}_2, \quad (5.18)$$

the integral over which can easily be shown to go to zero under the same condition as that for the fifth term. This concludes the proof that the only non-vanishing contribution to (5.9) in the limit $r \rightarrow \infty$ is due to the sixth term, i.e. the

pseudomomentum flux term. So, formally to all orders in ϵ , we have

$$\mathbf{R}_V = -\lim_{r \rightarrow \infty} \int_0^{2\pi} H \overline{\mathbf{u}'_1 \mathbf{u}'_1} \cdot \hat{\mathbf{n}} r \, d\theta = -\lim_{r \rightarrow \infty} \int_0^{2\pi} H \mathbf{p} \mathbf{u}_g \cdot \hat{\mathbf{n}} r \, d\theta. \quad (5.19)$$

This shows that the recoil force is equal to minus the difference between outgoing and incoming pseudomomentum fluxes. In other words, \mathbf{R}_V is equal to minus the rate of change of pseudomomentum due to refraction by the vortex flow. Though pseudomomentum is being changed, wave action is still conserved, and hence the total rate of change of pseudomomentum is equal to the change in wavenumber vector from one end of the wavetrain to the other, at $x = \pm\infty$, times the total flux of conserved wave action along the wavetrain:

$$\mathbf{R}_V = -(\mathbf{k}_B - \mathbf{k}_A) (\text{total wave-action flux along wavetrain}), \quad (5.20)$$

where \mathbf{k}_A and \mathbf{k}_B denote the asymptotically incoming and outgoing wavenumber vectors. As said before, this result is valid without restriction to a weak vortex, i.e. without restriction to $\epsilon \ll 1$.

We can now use (5.20) to compute the scattering angle at $O(\epsilon^2)$. Because the wavenumber change is $O(\epsilon^2)$, the wave-action flux need only be computed at $O(\epsilon^0)$, hence as

$$\text{total wave-action flux along wavetrain} = c_0 \int_{-\infty}^{+\infty} A_s(y) \, dy. \quad (5.21)$$

Because of the ray-invariance of absolute frequency we have that $|\mathbf{k}_A| = |\mathbf{k}_B|$ asymptotically. Hence \mathbf{k}_B must be a rotation of \mathbf{k}_A such that

$$\mathbf{k}_B - \mathbf{k}_A = \theta_* \hat{\mathbf{z}} \times \mathbf{k}_A \quad (5.22)$$

with small scattering angle θ_* . Now, using (5.7), (5.20), (5.22), and the fact that $\mathbf{k}_A = (k_0, 0)$, we obtain

$$\theta_* = \frac{\Gamma^2(\gamma + 2) \operatorname{sgn}(D)}{16\pi c_0^2 D^2} = \frac{\pi\epsilon^2(\gamma + 2) \operatorname{sgn}(D)}{4} \quad (5.23)$$

for the scattering angle at $O(\epsilon^2)$. The scattering is toward the vortex if $\gamma > -2$, as in figure 4 below, otherwise it is away from the vortex. Notice that (5.7) can now be rewritten

$$\mathbf{R}_V = -\hat{\mathbf{y}} \theta_* |\text{total pseudomomentum flux along wavetrain}|. \quad (5.24)$$

The direction of \mathbf{R}_V is not, of course, exactly parallel to $-\hat{\mathbf{y}}$, but rather makes an $O(\epsilon^2)$ angle $\frac{1}{2}\theta_*$ with the y -axis. As in (5.7) we have omitted the x component, $\propto \frac{1}{2}\hat{\mathbf{x}}\theta_*$, since its magnitude is $O(a^2\epsilon^4)$.

6. Numerical ray tracing

Numerical ray-tracing results are presented now that illustrate and test the theoretical $O(\epsilon^2)$ predictions obtained above. It is straightforward to integrate the full ray-tracing equations numerically, i.e. there is no need to restrict to small ϵ here. Recalling the standard ray-tracing equations (2.11), the local wave speed is

$$c(r) = c_0 \sqrt{H^{\gamma-1}} = c_0 \sqrt{1 - \frac{\gamma-1}{2} \frac{\tilde{U}^2}{c_0^2}}, \quad (6.1)$$

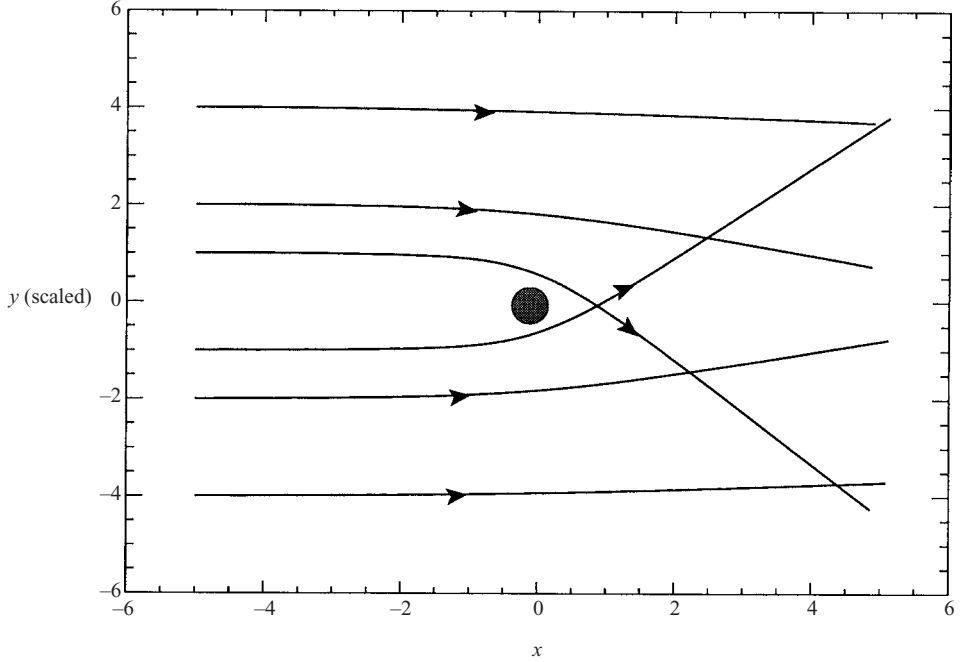


FIGURE 4. Numerical ray-tracing results for $\gamma = 1.4$ illustrating symmetric focusing of wave rays in the lee of the vortex. Rays are started from $|y_0| = \{4, 2, 1\}$ and the corresponding values of ϵ were $\{0.0125, 0.025, 0.05\}$. The y -axis is greatly stretched to show the scattering. Specifically, the individual plotted lines are $y_0 + (y(t) - y_0)/\theta_*$ where θ_* is the scattering angle (5.23) for $\epsilon = 0.05$. With this scaling the ray nearest to the vortex should be turned into the corners of the plot, as illustrated; the departure from this is due to the finite value of ϵ .

where as before \mathbf{U} is given by (4.4), $r = |\mathbf{x}|$, $\tilde{U}(r) = |\mathbf{U}|$, and $\kappa = |\mathbf{k}|$. Now, in (2.14) the term

$$\nabla c = \frac{dc}{d\tilde{U}} \frac{d\tilde{U}}{dr} \nabla r = \frac{\gamma - 1}{2} \frac{\tilde{U}^2}{c} \frac{(x, y)}{r^2} \quad (6.2)$$

by the chain rule. Using this result we obtain

$$\frac{d\mathbf{x}}{dt} = c \frac{\mathbf{k}}{\kappa} + \mathbf{U}, \quad (6.3)$$

$$\frac{dk}{dt} = -\frac{\gamma - 1}{2} \frac{\tilde{U}^2}{c} \frac{x}{r^2} \kappa - \frac{\Gamma}{2\pi} \left(\frac{2xy}{r^4} k + \frac{y^2 - x^2}{r^4} l \right), \quad (6.4)$$

$$\frac{dl}{dt} = -\frac{\gamma - 1}{2} \frac{\tilde{U}^2}{c} \frac{y}{r^2} \kappa + \frac{\Gamma}{2\pi} \left(\frac{2xy}{r^4} l - \frac{y^2 - x^2}{r^4} k \right), \quad (6.5)$$

which can be readily integrated with a standard Runge–Kutta scheme.

A typical scattering run starts from initial conditions $x(0) = -\infty$ (or rather a large enough negative number), $y(0) = -D$, $k(0) = k_0 > 0$, and $l(0) = 0$. Now, dimensional analysis of the ray-tracing system shows that after suitable scaling a ray trajectory can at most depend on three dimensionless parameters: γ , ϵ , and $k_0 D$. However, inspection reveals that $k_0 D$ is actually unimportant in these equations, and hence ϵ is the only relevant parameter at fixed γ . This implies that two trajectories with different D and Γ but equal ϵ are similar, e.g. they have the same scattering angle. Figure 4 shows

D	ϵ	θ_*	θ_r	$(\theta_* - \theta_r)/\theta_r$
0.2	0.25	0.17	0.14	0.21
0.5	0.10	0.027	0.024	0.12
1.0	0.05	0.0067	0.0063	0.065
5.0	0.01	0.00027	0.00026	0.014

TABLE 1. Scattering results for $\gamma = 1.4$. Only $y_0 = -D$ is varied between runs. The predicted scattering angle θ_* is taken from (5.23), the angle θ_r comes from the numerical integration. The relative error in the last column scales with ϵ .

the results of a number of runs with varying $y(0) = -D$, all other parameters being kept constant (in particular, $\gamma = 1.4$). The figure grossly exaggerates the scattering angles by rescaling the y -axis as described in the caption. The conspicuous symmetry between waves passing to the left of or to the right of the vortex can be clearly observed (cf. the far-field region in the analysis of Ford & Llewellyn Smith 1999): for $\gamma > -2$ the vortex focuses wave rays in its lee in a symmetric fashion.

The scattering angle θ_r was computed numerically for various values of ϵ and compared to the analytical predictions θ_* from (5.23). The results are collected in table 1. The relative error shown in the last column clearly scales as ϵ , which suggests that the next term in the expansion of θ_* would be $\propto \epsilon^3$. Such a term would hence break the symmetry between waves passing to the left or right of the vortex that holds at $O(\epsilon^2)$.

These scattering results were obtained by varying ϵ whilst keeping γ constant. Conversely, the variation of γ at fixed ϵ can lead to some surprising results in the appearance of the ray trajectory, especially for negative values of γ . Such negative values are perfectly acceptable from a mathematical point of view (cf. the discussion in Bühler 1998) because the pressure $p(h) = c_0^2 h^\gamma / \gamma$ is an increasing function of $h > 0$ for all γ . Surprisingly, it turns out that there is a range of $\gamma < 0$ for which the curvature along the ray can change sign, causing the ray trajectory to wiggle. Specifically, if $-2 < \gamma < -1$ then the waves are scattered toward the vortex — with overall or global bending of ray paths still as in figure 4 — even though the ray curves away from the vortex at the point of shortest distance of the wavetrain from the vortex.

This can be demonstrated by computing the curvature of the ray trajectory at the point of shortest distance to the vortex, taken to be $x = (0, -D)$ for convenience and without loss of generality. The ray is almost a horizontal line $y = \text{const.}$ near this point, hence dy/dx is small and the geometric ray curvature can be approximated by

$$\frac{d^2y}{dx^2} = \frac{d}{dx} \frac{dy}{dx} = \frac{1}{u_g} \frac{d}{dt} \left(\frac{v_g}{u_g} \right) = \frac{1}{u_g} \left(\frac{1}{u_g} \frac{dv_g}{dt} - \frac{v_g}{u_g^2} \frac{du_g}{dt} \right). \quad (6.6)$$

This expression can be simplified by using that $v_g = 0$ and $V = 0$ at this point, which together imply that $l = 0$ there as well. This means the last term in (6.6) is zero and furthermore

$$\frac{dv_g}{dt} = \frac{d}{dt} \left(c \frac{l}{k} + V \right) = \frac{c}{k} \frac{dl}{dt} + \frac{\partial V}{\partial x} u_g = \frac{c}{k} \left(\frac{\gamma - 1}{2} \frac{U^2}{c} \frac{k}{D} - \frac{\Gamma}{2\pi D^2} \frac{k}{D} \right) + \frac{\Gamma}{2\pi D^2} u_g \quad (6.7)$$

using $k = \kappa > 0$. Substituting in (6.6) and truncating at $O(\epsilon^2)$ then produces a ray

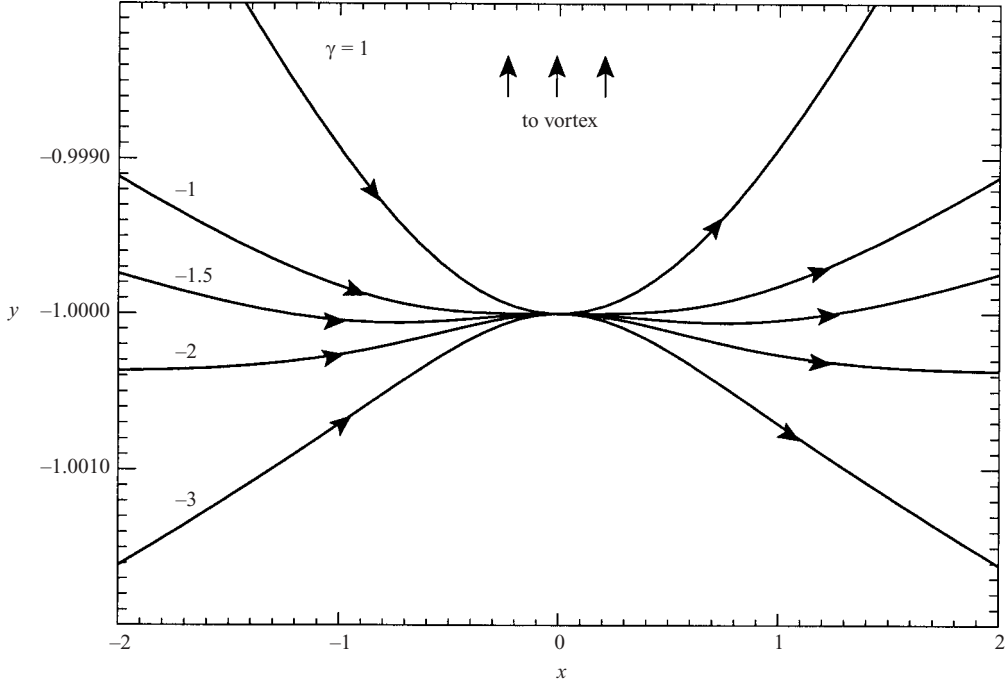


FIGURE 5. Zoom of trajectory details at the point nearest to the vortex. From top to bottom of the picture, rays with five different values of γ are shown; ϵ is always the same. The $\gamma = 1$ ray has positive curvature at the point nearest to the vortex and is scattered toward the vortex. The $\gamma = -1$ ray (non-steepening model) has zero curvature at this point (cf. (6.8)). The $\gamma = -1.5$ ray has negative curvature locally but is still scattered toward the vortex eventually; this ray has a wiggle. At $\gamma = -2$ there is zero scattering (cf. (5.23)), and at $\gamma = -3$ the curvature and scattering are both negative.

curvature of

$$\frac{\gamma+1}{2D} \left(\frac{\Gamma}{2\pi D c_0} \right)^2 = \frac{\gamma+1}{2D} \epsilon^2 \quad (6.8)$$

at the point nearest to the vortex. A positive sign (for $D > 0$) corresponds to curvature toward the vortex here.

Now, this curvature changes sign at $\gamma = -1$, which is a different threshold than the global scattering threshold $\gamma = -2$. In other words, in the range $-2 < \gamma < -1$ the global scattering is still toward the vortex whilst the local curvature at the point closest to the vortex now points away from it. This is illustrated by a few trajectories at various γ in figure 5; see caption for details. In particular, the middle trajectory has $\gamma = -1.5$ and one can see that global scattering toward the vortex is achieved whilst bending away from the vortex near $x = (0, -D)$. Of course, only the global scattering angle matters for the global momentum budget and hence for the net vortex recoil.

7. Concluding remarks

The idealized problems studied in this paper have clearly shown the nature of the new wave-vortex effect: a pseudomomentum change due to wave refraction by a horizontally inhomogeneous background flow goes hand-in-hand with a recoil felt by the mean flow. In the present case this could be represented as an effective recoil

force felt by the vortex core, evoking, in turn, far-field ‘pressure at infinity’ recoil effects of the kind encountered in classical vortex-impulse studies. The effective recoil force on the core is equal and opposite to the rate of change of the waves’ pseudomomentum due to refraction by the vortex, superficially in accordance with a naive ‘photon analogy’ that conflates pseudomomentum with momentum. But the photon analogy would say that the force is felt within the refracting wavetrain, rather than in the vortex core, which latter is located well away from the wavetrain in the parameter regime studied. We stress yet again that, for a steady wavetrain continually propagating past the vortex, the effective recoil force is persistent, and cumulative in time.

The formal asymptotics used here is sufficient to reveal all the essential features of the problem, even though improved asymptotic schemes suggest themselves, for instance based on transformed coordinates whose origin follows the persistently translating vortex core, thus extending the range of validity in time.

As far as we are aware, this has been the first study of horizontally refracted waves that computes the concomitant $O(a^2)$ mean-flow response at sufficient accuracy to make definite statements about the momentum and pseudomomentum budgets and hence about the recoil forces. Furthermore, the explicit formula (5.23) for the leading-order scattering angle of a wavetrain passing a vortex at a distance emerged as a by-product of this study. Whilst similar results might be well known to some researchers, we are unaware of an explicit formula for this scattering angle elsewhere in the literature. It is related to the effective recoil force \mathbf{R}_V by (5.24).

The highly idealized nature of the problem studied here, a single weak vortex with potential flow outside it, allowed a fairly complete analysis of the flow with moderate effort. Despite the idealizations, we suggest that the recoil effect described is robust in its essential features. For instance, replacing the perfectly irrotational wave sink with a local region of wave dissipation (e.g. Bühler 2000) would change only the local details of the mean-flow computation at the wave sink. The remote recoil effects would still be present, just as described here.

For the infinite wavetrain, the Magnus relation (4.15) reminds us that the remote recoil effects come from advection of the vortex core by the $O(a^2)$ mean flow that the refracting wavetrain induces in its surroundings. It is crucial, in the present case, that only the vortex core is advected and not the periphery or far field of the vortex. This is related to the fact that the fourth term in (5.9) can be neglected as $r \rightarrow \infty$, for the narrow wavetrain assumed. In other words the recoil effects, including the unsteady far-field recoil discussed in § 4.4, arise precisely from the vortex core being moved relative to the vortex periphery. Of course the effective force \mathbf{R}_V that must be applied, persistently, to the vortex core, to produce the same cumulative effects in the absence of the waves, does precisely the same thing. It moves the vortex core without advecting the vortex periphery. Recall that the sense of the core advection, and with it the sense of \mathbf{R}_V , is opposite to that in figure 3, owing to the bending of the infinite wavetrain.

Generalizing the present study to more realistic cases of greater geophysical relevance is an aim for future work. Within the shallow-water system the obvious next step is to allow for non-zero Coriolis forces, i.e. non-zero Coriolis parameter f , using the natural definition of the vortex core as an anomaly in potential vorticity instead of vorticity. This will change the nature of the background vortex flow by modifying its $1/r$ far-field velocity tail to a tail decaying exponentially like $\exp(-r f/c_0)$. On the one hand, this greatly reduces the background velocity available for refraction; on the other hand the background velocity now has non-zero curl even in the far

field, which increases the refraction because wave rays are then not straight lines at leading order in Froude or Mach number. This could make for an interesting competition of effects for non-zero f . Another direction for generalization is to allow for several vortices, or even for a turbulent background flow, which presumably would have been treated statistically. It seems clear, moreover, that for complex background vortex structures the identification of the recoil force with minus the rate of change of pseudomomentum can hold in a global, domain-integrated sense only. In other words, the effective recoil felt by any particular vortex will depend not only on the wavetrain but also on the presence of all the other vortices. As far as we can see, the way in which the recoil is distributed between the vortex cores is not obvious without detailed analysis. One might hope to find a simple statistical-mechanical rule, but so far no such rule has been found.

Outside the shallow-water system the next target is the three-dimensional stratified Boussinesq system, in which the longitudinal shallow-water waves are replaced by transverse internal-gravity waves. We fully expect the main features of the present theory to carry over to that case, when stated as above with the central role given to the pseudomomentum \mathbf{p} per unit mass rather than to the Stokes drift $\bar{\mathbf{u}}^s$. Although the two entities coincide in the shallow-water problem, as implied by (2.17), they become distinct in the stratified problem, with \mathbf{p} remaining significant but $\bar{\mathbf{u}}^s$ becoming irrelevant. This primacy of \mathbf{p} over $\bar{\mathbf{u}}^s$ was already implicit in the work of Bretherton (1969), and has emerged very plainly from more recent work using a generalized Lagrangian-mean framework (Bühler & McIntyre 1998). Progress on the stratified remote-recoil problem is being made, and we hope to report on it in the meteorological literature very soon.

Clearly, the remote recoil effects described here imply a major, qualitative change in the paradigm for horizontally (latitudinally and longitudinally) homogeneous background flows on which all present gravity-wave parametrization schemes are built; again see the two recent reviews already cited (Fritts & Alexander 2003; Kim *et al.* 2003). Indeed, the remote recoil effect undoes the conventional link between the force felt at the wave source (e.g. the wave drag on a mountain range) and the force felt at the dissipative wave sink (usually involving wave breaking in the stratosphere or mesosphere, anywhere from 10 km upwards). These forces need not be equal and opposite: Newton's third law is realized in a much more complicated way.

We thank colleagues for helpful comments and correspondence, also the referees for constructive comments that have prompted us to highlight certain issues more clearly and to generalize significantly the results of § 5.2, and the UK Natural Environment and Science and Engineering Research Councils for generous support including a SERC/EPSRC Senior Research Fellowship.

REFERENCES

- ANDREWS, D. G. & MCINTYRE, M. E. 1978 On wave-action and its relatives. *J. Fluid Mech.* **89**, 647–664, and Corrigendum **95**, 796; also **106**, 331.
- BOOKER, J. R. & BRETHERTON, F. P. 1967 The critical layer for internal gravity waves in a shear flow. *J. Fluid Mech.* **27**, 513–539.
- BRETHERTON, F. P. 1969 On the mean motion induced by internal gravity waves. *J. Fluid Mech.* **36**, 785–803.
- BRETHERTON, F. P. & GARRETT, C. J. R. 1968 Wavetrains in inhomogeneous moving media. *Proc. R. Soc. Lond. A* **302**, 529–554.
- BRILLOUIN, L. 1925 On radiation stresses. *Ann. Physique* **4**, 528–586 (in French).

- BÜHLER, O. 1998 A shallow-water model that prevents nonlinear steepening of gravity waves. *J. Atmos. Sci.* **55**, 2884–2891.
- BÜHLER, O. 2000 On the vorticity transport due to dissipating or breaking waves in shallow-water flow. *J. Fluid Mech.* **407**, 235–263.
- BÜHLER, O. & JACOBSON, T. E. 2001 Wave-driven currents and vortex dynamics on barred beaches. *J. Fluid Mech.* **449**, 313–339.
- BÜHLER, O. & MCINTYRE, M. E. 1998 On non-dissipative wave–mean interactions in the atmosphere or oceans. *J. Fluid Mech.* **354**, 301–343.
- DONNELLY, R. J. 1991 *Quantized Vortices in Helium II*. Cambridge University Press.
- DYSTHE, K. B. 2001 Refraction of gravity waves by weak current gradients. *J. Fluid Mech.* **442**, 157–159.
- ELIASSEN, A. & PALM, E. 1961 On the transfer of energy in stationary mountain waves. *Geophys. Publ.* **22**(3), 1–23.
- FEYNMAN, R. P. 1998 *Statistical Mechanics*. Addison-Wesley.
- FORD, R. & LLEWELLYN SMITH, S. G. 1999 Scattering of acoustic waves by a vortex. *J. Fluid Mech.* **386**, 305–328.
- FRITTS, D. C. & ALEXANDER, M. J. 2003 Gravity-wave dynamics and effects in the middle atmosphere. *Revs. Geophys.* **41**(1), doi: 10.1029/2001RG000106.
- JONES, W. L. 1967 Propagation of internal gravity waves in fluids with shear flow and rotation. *J. Fluid Mech.* **30**, 439–448.
- KIM, Y.-J., ECKERMAN, S. D. & CHUN, H.-Y. 2003 An overview of the past, present and future of gravity-wave drag parametrization for numerical climate and weather prediction models. *Atmos.–Ocean* **41**, 65–98.
- LAMB, H. 1932 *Hydrodynamics*, 6th edn. Cambridge University Press.
- LANDAU, L. D. & LIFSHITZ, E. M. 1987 *Fluid Mechanics*, 2nd Engl. Edn, Pergamon.
- LONGUET-HIGGINS, M. S. 1977 The mean forces exerted by waves on floating or submerged bodies with applications to sand bars and wave power machines. *Proc. R. Soc. Lond. A* **352**, 463–480.
- LONGUET-HIGGINS, M. S. & STEWART, R. W. 1964 Radiation stress in water waves; a physical discussion, with applications. *Deep-Sea Res.* **11**, 529–562.
- LÜBKEN, F.-J. 1999 Thermal structure of the Arctic summer mesosphere. *J. Geophys. Res.* **104**, 9135–9149.
- MCINTYRE, M. E. 1981 On the ‘wave-momentum’ myth. *J. Fluid Mech.* **106**, 331–347.
- MCINTYRE, M. E. 2003 On global-scale atmospheric circulations. In *Perspectives in Fluid Dynamics: A Collective Introduction to Current Research* (ed. G. K. Batchelor, H. K. Moffatt, M. G. Worster), pp. 557–624. Cambridge, University Press. (Paperback edition, with important corrections.)
- PALMER, T. N., SHUTTS, G. J. & SWINBANK, R. 1986 Alleviation of a systematic westerly bias in general circulation and numerical weather prediction models through an orographic gravity wave drag parametrization. *Q. J. R. Met. Soc.* **112**, 1001–1039.
- RAYLEIGH, LORD 1896 *The Theory of Sound*, Vol. 2. Dover (reprinted 1945).
- THOMAS, G. E., OLIVERO, J. J., JENSEN, E. J., SCHRÖDER, W. & TOON, O. B. 1989 Relation between increasing methane and the presence of ice clouds at the mesopause. *Nature* **338**, 490–492.
- WHITHAM, G. B. 1974 *Linear and Nonlinear Waves*. Wiley-Interscience.